FEATURE ARTICLE

The Energy Landscape of Myoglobin: An Optical Study

Daan Thorn Leeson and Douwe A. Wiersma*

Ultrafast Laser and Spectroscopy Laboratory, Department of Chemistry and Materials Science Center, University of Groningen, Nijenborgh 4, 9747 AG, Groningen, The Netherlands

Klaus Fritsch and Josef Friedrich

Technische Universität München, Lehrstuhl für Physik, Weihenstephan, D-85350 Freising, Germany

Received: March 13, 1997; In Final Form: June 2, 1997[⊗]

In this paper we demonstrate how the potential energy surface of a protein, which determines its conformational degrees of freedom, can be constructed from a series of advanced nonlinear optical experiments. The energy landscape of myoglobin was probed by studying its low-temperature structural dynamics, using several spectral hole burning and photon echo techniques. The spectral diffusion of the heme group of the protein was studied on a time scale ranging from nanoseconds to several days while covering a temperature range from 100 mK to 23 K. The spectral line broadening, as measured in three-pulse stimulated photon echo experiments, occurs in a stepwise fashion, while the exact time dependence of the line width is critically dependent on temperature. From these results we obtained the energy barriers between the conformational states of the protein. Aging time dependent hole-burning experiments show that, at 100 mK, it takes several days for the protein to reach thermal equilibrium. When, after this period a spectral hole is burned, the line broadening induced by well-defined temperature cycles is partly reversed over a period of several hours. From this we conclude that a rough structure is superimposed on the overall shape of the potential energy surface of the protein. By combining the hole burning and photon echo results, we construct a detailed image of this energy landscape, supporting the general concept of a structural hierarchy. More specifically, we show that the number of conformational substates in the lower hierarchical tiers is much lower than was previously anticipated and, in fact, is comparable to the number of taxonomic substates.

1. Introduction

Protein function requires a delicate balance between structural order and structural disorder. Order is reflected in the fact that proteins have well-defined tertiary structures. The relation between the three-dimensional structure of a protein and its biochemical function is a key concept in structural biology, and its existence is supported by many examples. However, the functioning of a protein cannot be understood solely in terms of its three-dimensional structure. The missing link is structural disorder. Disorder in proteins manifests itself in structural indeterminism and structural dynamics. Structural indeterminism means that the structures of individual protein molecules out of an ensemble are slightly different. Proteins are dynamic systems in the sense that the structure of a single molecule fluctuates on a broad range of time scales. Therefore, three-dimensional structures, as determined by X-ray diffraction or nuclear magnetic resonance, should be considered as an average, either an ensemble average or the time average of a single protein. In some cases the connection between function and disorder is straightforward. An example is the entrance and exit of small ligands in myoglobin, which requires a conformational rearrangement of the protein.[1] However, in general, much remains to be learned. To arrive at a better understanding, one needs to map out the conformational degrees of freedom of proteins and characterize their energy landscapes (ELs). The term EL refers to the potential energy hypersurface that is spanned by the relative coordinates of the atoms in a protein. All conformational dynamics of a protein ranging from the folding into its native structure to local atomic fluctuations correspond to the diffusion of a point, representing the structure at a particular instant, within this potential. Therefore, knowledge of the detailed structure of the ELs of proteins will contribute to our understanding of protein function. For instance, the power of the EL metaphor is illustrated by recent developments in the treatment of protein folding.[2] The concept of an EL is further illustrated in Figure 1. Due to the large number of coordinates, the aperiodic nature of a protein structure, and the various types of interactions that determine its energy, the ELs of proteins are extremely complex. In spite of this inherent complexity it is still possible to give a global description of the EL based on simple energetic and structural arguments. Descriptions of protein ELs are usually one-dimensional, which can be interpreted as the projection of a single, generalized, coordinate out of the multidimensional conformational phase space or as a one-dimensional cross section. The overall shape of the EL is that of a steep well. Because the native structure is well-defined, it should have an energy much lower than that of the unfolded protein, or other possible conformations. Superimposed on the well shape is a rugged structure that exists on a broad range of energy and length scales. Ruggedness essentially arises from structural frustration. The compact structure of a protein requires certain atoms or functional groups to be in close contact. Not all

[⊗] Abstract published in *Advance ACS Abstracts,* July 15, 1997.

S1089-5647(97)00908-5 CCC: $14.00

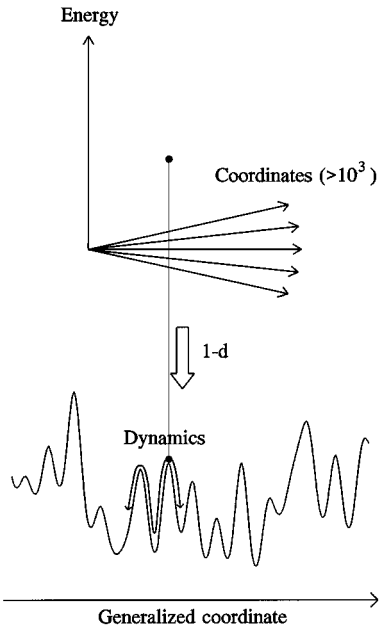

Figure 1. Schematic representation of the concept of an energy landscape.

interactions can be energetically favorable, and hence, the protein is structurally frustrated. The native conformation is a structural compromise with a maximal number of favorable and a minimal number of unfavorable interactions. The low-energy part of the EL, which characterizes the dynamics of the native state, i.e. the functioning state of the protein, is dominated by the rugged structure. It comprises a large number of local minima, which correspond to nearly degenerate conformational substates (CSs).[3] CSs have the same overall structure but are slightly different on a more detailed level.[4] Although the concept of CSs is based on experiments performed on myoglobin, more recent developments show that it is much more widely applicable.[5,6] However, myoglobin remains an attractive model system. On the basis of the multitude of work done so far on myoglobin, it is the most likely candidate to be the first to have its EL described in detail. For instance, an important question is whether the ELs of proteins are hierarchically organized, as was proposed by Frauenfelder and co-workers.[7] CSs are assumed to exist on a number of hierarchical tiers, where each tier is characterized by an average energy barrier between the CSs. Descending within the hierarchy, the barriers between CSs, as well as the average mean atomic displacements between them, decrease. The consequence of this model is that also the structural dynamics of the system are hierarchically organized. On long time scales the protein will exhibit large-scale, most likely global, fluctuations, while on shorter time scales, lower amplitude, possibly local motions occur. An essential variable to test this model is temperature. By lowering the temperature one can freeze out the large-scale motions, which require the crossing of large energy barriers, and study the motions within the lower hierarchical tiers. The aim of this paper is to demonstrate how advanced optical techniques can be applied to arrive at a detailed description of the EL of a protein by performing a number of optical line narrowing experiments on myoglobin. The power of the techniques lies in the extremely broad dynamic range. Experiments were performed between 100 mK and 23 K, while covering a time window from nanoseconds to several days.

2. Optical Line Narrowing Spectroscopy

The experiments presented in this paper rely on the fact that the resonance frequencies of the optical transitions of the

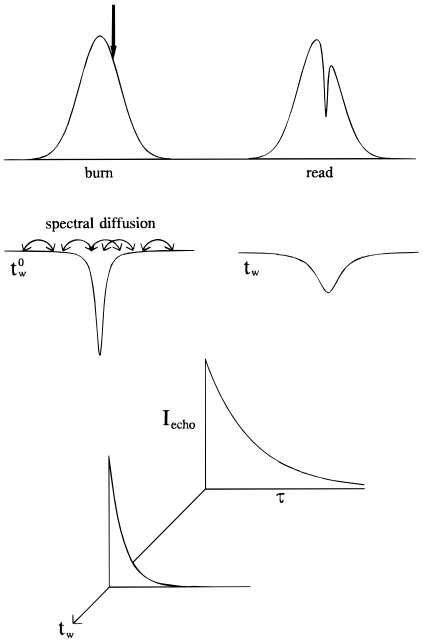

Figure 2. Upper part: Description of a spectral hole burning experiment. Middle part: Schematic representation of the effect of spectral diffusion (represented by the double-sided arrows) on the spectral line width. Lower part: The corresponding effect on the 3PSE decay.

chromophore in a chromoprotein are influenced by the conformational state of the protein. Hence, the resonance frequency of a particular transition can serve as a marker for the protein structure at a certain instant, and conformational changes will cause it to fluctuate. The fluctuations of optical frequencies of chromophores that are induced by structural changes of its host are referred to as spectral diffusion (SD). The study of SD can yield vital information on the conformational dynamics of proteins and related systems, such as glasses and polymers. Due to the structural indeterminism, optical absorption spectra of chromoproteins are strongly inhomogeneously broadened. Therefore, in order to measure SD, one needs to remove the inhomogeneous broadening from the spectrum. Techniques that can do this fall within the field of optical line narrowing spectroscopy. Examples are single-molecule spectroscopy, fluorescence line narrowing spectroscopy, spectral hole burning (SHB), and photon echo (PE). In this paper we apply SHB and PE to study SD in myoglobin. SHB and PE are complementary techniques in the sense that PE is the time domain equivalent of SHB. Since SHB and how it can measure SD are much more straightforward to explain, we will restrict ourselves for the remainder of this paper to the frequency domain, making only brief references to the PE experiment.

Figure 2 describes a SHB experiment. In a SHB experiment a narrow band laser field is applied to a sample with an inhomogeneously broadened spectrum. The chromophores that have been excited by the laser field are transformed into a photochemical or photophysical product state. As a consequence, these molecules will no longer absorb at the transition on which they were excited, and a hole, centered at the laser frequency, appears when the spectrum is recorded. The width of the spectral hole is twice the homogeneous line width, which is determined by the optical dephasing time of the transition involved. For a more detailed review of SHB see ref 8. The time domain equivalent of this experiment is the three-pulse stimulated photon echo (3PSE).[9] In a 3PSE experiment a coherent signal is generated after a sequence of three picosecond optical pulses. The decay of the signal as a function of the time separation of the first two pulses corresponds to the Fourier

transform of the spectral hole width, where the time separation of the second and the third pulse corresponds to the time between burning and reading the spectral hole, as is illustrated in Figure 2. During this time, referred to as the waiting time, t_w, individual chromophores can wander in frequency space. Fluctuations can be induced by the equilibrium structural dynamics of the host matrix or by changing external variables such as temperature, pressure, or electric field, during t_w. The influence of SD on the line shape is also illustrated in Figure 2. The line shape, $\Gamma(\omega)$, at $t = t_w^0$, serves as a marker for the conformational state of the system at this instant. The line shape at longer t_w is related to the initial line shape through the relation

$$\Gamma(\omega,t_w) = \int_{-\infty}^{\infty} d\omega(t_w^0)\, \Gamma(\omega,t_w^0)\, P[\omega(t_w) - \omega(t_w^0)] \quad (1)$$

Here $P[\omega(t_w) - \omega(t_w^0)]$ is the distribution over the ensemble of chromophores of the difference in resonance frequency between t_w and t_w^0. It is a measure for the conformational changes that have occurred during this time interval.

A. Waiting Time Dependent Spectral Diffusion Experiments. In these experiments, the dependence of the line width on t_w is measured at fixed temperature, when the system is in thermal equilibrium. The equilibrium structural dynamics of the protein induces SD, which causes $P[\omega(t_w) - \omega(t_w^0)]$ and, consequently, the line width to broaden when t_w is increased. Since the dynamics are determined by the structure of the EL, specific information, such as the height and distribution of the energy barriers, can be obtained from the t_w dependence of the line width. A quantitative description of SD in structurally disordered materials has been given by Bai and Fayer,[10] who based their work on the so-called sudden jump model of Hu and Walker.[11] The model assumes that the resonance frequencies of the ensemble of chromophores are influenced by a number of fluctuating perturbers. Each perturber fluctuates between two states at a particular rate, R. Transitions between the two states occur instantly, and R is defined as the inverse of the average time between two sudden jumps. When the perturber changes its state, it induces a small shift of the resonance frequencies of the chromophores it is coupled to. The combined action of the total number of perturbers on the ensemble of chromophores causes the line width to increase as a function of t_w. The exact time dependence is determined by the distribution of fluctuation rates $P(R)$. Bai and Fayer showed that the t_w dependence of the line width, Γ, is related to $P(R)$ in the following way:

$$\Gamma(t_w) = \Gamma(t_w^0) + \int_0^{\infty} dR\, P(R)[\exp(-Rt_w^0) - \exp(-Rt_w)] \quad (2)$$

The connection between this approach and the structure of the EL is the so-called two-level-system (TLS) model.[12,13] The TLS model assumes that the EL can be represented by a number of double- well potentials, the TLSs. The wells of a TLS correspond to two distinct configurations of a localized structural element of the system that are separated by an energy barrier. Within the sudden jump model the TLSs are represented by the perturbers; that is, SD is induced by transitions between the two states of the TLSs. The energy barrier can be crossed either by tunneling or thermal activation. Therefore, $P(R)$ is determined by the distribution of the barrier heights and asymmetries of the TLSs that comprise the system. The TLS model has been very successful in describing the optical properties of impurity doped glasses[14] and has also been applied to proteins.[15−18] However, the question of whether it gives a proper representation of the EL of a protein has not been satisfactorily answered. One of the goals of the paper is to address this problem.

B. Aging Time Dependent Spectral Diffusion Experiments. At sufficiently low temperatures, structurally disordered materials like glasses and polymers but also proteins can be far from thermal equilibrium. For temperatures below 1 K it appears that even relaxation toward local equilibrium takes an extremely long time. If the protein is not in equilibrium and relaxation occurs on the time scale of the experiment, there will be an additional contribution to the line broadening due to the downward traveling of the protein on its EL. The deviation from thermal equilibrium is measured by the parameter, t_a, the so-called aging time. This is the time elapsed after the experimental temperature has been reached. In an aging time spectral diffusion experiment the dependence of the line width on t_w is measured as a function of t_a. If the protein is relaxing toward equilibrium, the corresponding contribution to the line broadening should decrease when t_a is increased. Once (local) equilibrium has been established, the line-broadening behavior should no longer depend on t_a.

C. Temperature Cycling Spectral Diffusion Experiments. In these experiments a cyclic temperature variation is applied during t_w, or right before burning a spectral hole. The experimental parameters are the temperature at which the hole is burned and measured, the excursion temperature, T_e, which is the maximum temperature reached during the cycle, and the time, t_e, during which the sample is at the excursion temperature. During t_e the protein is able to cross energy barriers that are not surpassable at the burning temperature. The corresponding structural changes cause a broadening of the line width relative to its value in the absence of a temperature cycle. Measuring the line width as a function of T_e at fixed t_e yields information on the distribution of energy barriers within the EL, similar to t_w dependent measurements at fixed temperature.

Temperature cycling experiments can also be combined with waiting time dependent measurements.[19] Once equilibrium has been established, for instance by performing an aging time SD experiment, a temperature cycle to a specified excursion temperature allows one to create a well-defined nonequilibrium state. The subsequent relaxation toward equilibrium is measured through the time evolution of two spectral holes, hole A and hole B. Hole A is burned right before the temperature cycle, labeling the protein in its equilibrium state. Hole B is burned right after the temperature cycle and hence marks the nonequilibrium state of the protein. We will show that on the basis of the time evolution of these two holes one can obtain information on both qualitative and quantitative features of the potential energy surface.

3. Experimental Section

The PE and SHB experiments were both performed on apomyoglobin, complexed to either Zn−mesoporphyrin IX (Zn-mb) or free base protoporphyrin IX (H_2-mb). Samples were dissolved in a 3/1 v/v glycerol/water mixture, degassed, and sealed in 1 mm cuvettes. The optical densities at the excitation wavelengths were between 0.2 and 0.3. Comparative experiments on a glass were performed using the same chromophores (Zn-MP and H_2-PP) in glycerol with added dimethylformamide to ensure solubility.

The experimental setup to generate the sequence of optical pulses applied in the 3PSE experiments has been described in great detail.[20] Typically, the pulses have a duration of 5 ps and a spectral bandwidth of 8 cm^{-1}. The excitation wavelength was 578 nm. Pulse energies were typically 20 nJ. Samples were precooled by plunging them into liquid nitrogen and further

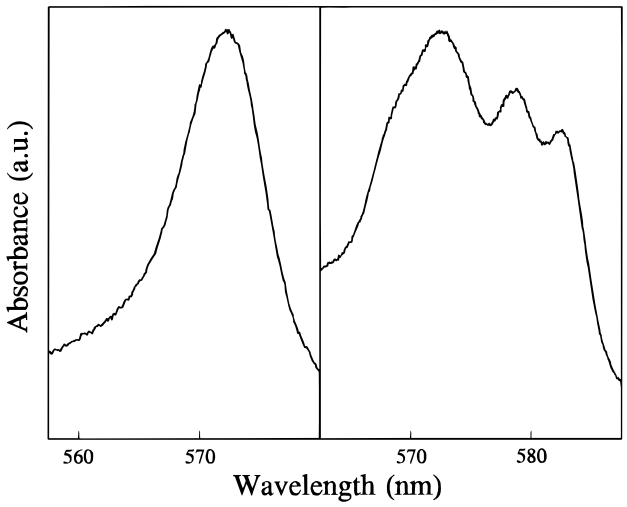

Figure 3. Linear absorption spectra, recorded at 77 K, of Zn-MP in 3/1 v/v glycerol/dimethylformamide (left-hand side) and Zn-mb (right-hand side).

cooled to the desired temperature in a helium bath cryostat. Samples were allowed to relax for at least 2 h at the experimental temperature before performing the experiments.

The experimental setup used in the SHB experiments has been described before.[21] Typical hole-burning times and powers were on the order of 2 min and 150 nW cm^{-2}, respectively. Hole burning was performed at 625 nm. Cooling to the millikelvin range was performed with a dilution refrigerator.

4. Results and Discussion

A. The Interaction of the Chromophore with Its Environment. All of the experiments discussed in the previous section are based on the same concept, that is to gain information on the dynamic properties of a protein by using its optical center as a probe in spectroscopic experiments. A consequence of this idea is that only those processes can be observed that modify the interaction of the chromophore with its environment. This means that optical experiments do not necessarily probe all the motions of the protein. As such, we cannot state with complete certainty that all the aspects of the protein's energy landscape will be revealed. However, this is true for any experiment, and obviously, a full understanding will have to emerge from a wide range of experiments.

The interaction of the chromophore with its environment can be short-ranged as well as long-ranged. Since the protein is dissolved in a glassy matrix, the question arises how sensitive the chromophore is to the solvent. If a strong coupling between the chromophore and the solvent exists, our experiments would probe not only the protein but also its host. This question cannot be readily answered using general arguments since it not only concerns the range of the relevant interactions but also depends on to what extent the strain and/or electric fields generated by the host matrix can penetrate the protein.

Specific information on the interaction of the chromophore with its environment can be obtained from a series of comparative experiments between chromoproteins and systems where the chromophore was directly dissolved in a glassy matrix. The simplest of such experiments is linear absorption spectroscopy. Figure 3 displays spectra, obtained at 77 K, of Zn-mb and of Zn-MP in a glass of glycerol and dimethylformamide. While the glassy solution exhibits only a single inhomogeneously broadened band, the protein spectrum comprises at least three bands, which most likely correspond to the different taxonomic CSs of myoglobin.[22] As such, Figure 3 shows that the heme

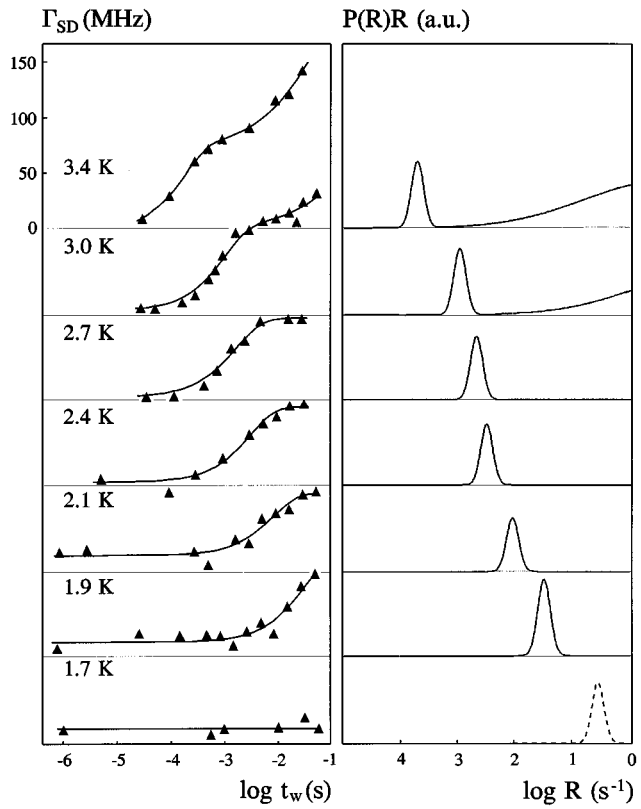

Figure 4. Line width vs t_w for Zn-mb (left-hand side). The solid lines through the data are fits to eq 2, using the distributions displayed on the right-hand side.

resonance frequency is strongly influenced by the conformational state of the protein. Hole-burning Stark-effect experiments[23,24] clearly demonstrate that a protein environment can break the symmetry of the chromophore by inducing a well-defined dipole moment. If there is a strong influence from the the random glass matrix, the induced dipole moment is random as well, and globally the symmetry is not broken. Furthermore, comparative SD experiments show qualitatively different behavior for glasses and proteins on one hand[25] and for different proteins on the other.[26] This clearly demonstrates that these experiments exclusively probe the protein, at least on the time scales relevant to this study. For SD experiments this is particularly surprising since the interactions are supposed to be of long range. The reason why the optical center is strongly shielded from the host matrix is not quite clear. Most probably, this is a result of the difference in magnitudes between the glass and the protein of the relevant material parameters, namely, the compressibility and the dielectric constant.

B. Three-Pulse Stimulated Photon Echo Experiments: Measuring Energy Barriers. Figure 4 shows the t_w dependence of the line width of Zn-mb in the region between 1 μs and 100 ms, for temperatures between 1.7 and 3.4 K. Plotted is Γ_{SD}, which is defined as

$$\Gamma_{SD} = \Gamma(t_w) - \Gamma(t_w^0) \tag{3}$$

where t_w^0 is the shortest waiting time measured.

At 1.7 K no line broadening is observed within this time window. However, at 1.9 K there is an increase of the line width in the millisecond region. As the temperature is further increased, the line broadening starts off at shorter t_w, while at 2.7 K it levels off in the millisecond region. This means that the line broadening occurs within a short time interval, while the time scale on which it occurs shifts with temperature. Before

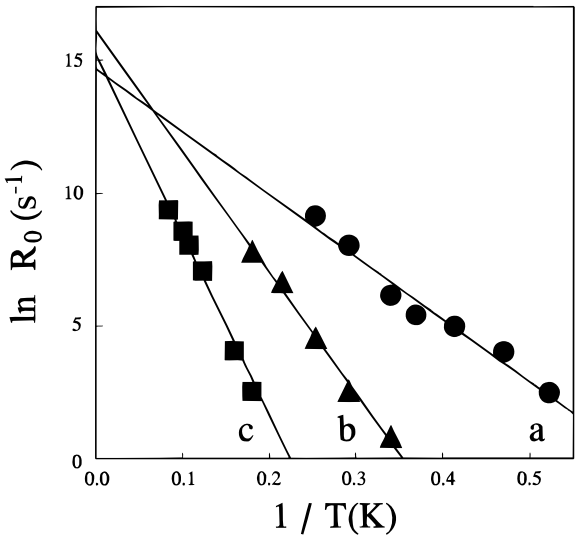

Figure 5. Temperature dependence of the fluctuation rates, R_0, corresponding to the centers of the rate distributions obtained from fits of line broadening data on Zn-mb as shown in Figures 4 and 6. The solid lines are fits to an Arrhenius law.

further analyzing this result, one can make a general phase space argument. The leveling off of the line broadening implies that the accessible frequency space of each chromophore is restricted. It corresponds to the situation where the time scale of the experiment is much longer than the time scale at which the chromophores explore this part of their frequency space. Because there is a relation between the resonance frequency of the optical center and the conformation of the protein, the experimental result implies that the protein is exploring a restricted part of its conformational phase space and is doing so on a sharply defined time scale. The solid lines in Figure 4 are fits of the data to eq 2, yielding a narrow distribution of fluctuation rates. In Figure 5 the natural logarithm of the fluctuation rate, R_0, corresponding to the center of each of the distributions of Figure 4 is plotted as a function of the inverse of the temperature. The data follow an Arrhenius law, i.e. $R_0 = A \exp(-E/kT)$, suggesting that the conformational rearrangements that cause the line broadening to occur via thermally activated barrier crossing. A linear fit yields a barrier height of 0.20 kJ mol^{-1} (16 cm^{-1}). The data at 3.0 and 3.4 K show an additional contribution to the line broadening in the millisecond region. More insight into the SD behavior is obtained by expanding the temperature range. Figure 6 shows the t_w dependence of the line width between 10 ns and 100 ms for temperatures between 3.0 and 23 K. Figure 6 once more shows that the t_w dependence of the line width is critically dependent on temperature. As was discussed above, the data between 1.7 and 3.4 K can be understood by assuming at least one narrow distribution of fluctuation rates, which we now denote as *a*. At 3.0 K feature *a* can be clearly resolved. Furthermore, reactivation of the line broadening in the millisecond region points toward the presence of additional features in the rate distribution. From the data at 4.7 K we conclude that a second feature, denoted as *b*, behaves identically as feature *a* in the sense that it is also a relatively narrow distribution that shifts with temperature. At 4.7 K feature *b* has shifted far enough into the direction of larger rates, so that we can observe the leveling off of the line broadening in the millisecond region just as we did for feature *a* at 2.7 K. The data at intermediate temperatures, although not shown here, are completely consistent with this picture. The data at 5.6 and 8.1 K show a remarkable similarity with those at 3.0 and 4.7 K. The data at 5.6 K supply evidence for a third feature in the rate distribution, denoted as *c*, as can

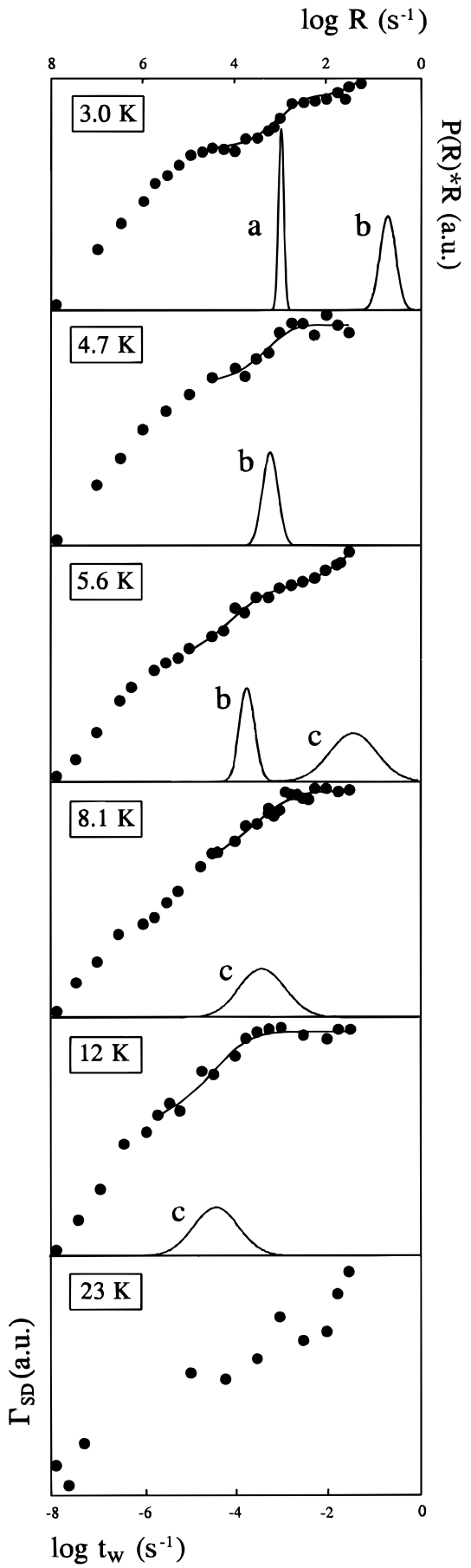

Figure 6. Line width vs t_w for Zn-mb. The solid lines through the data are fits to eq 2, using the distributions that are displayed.

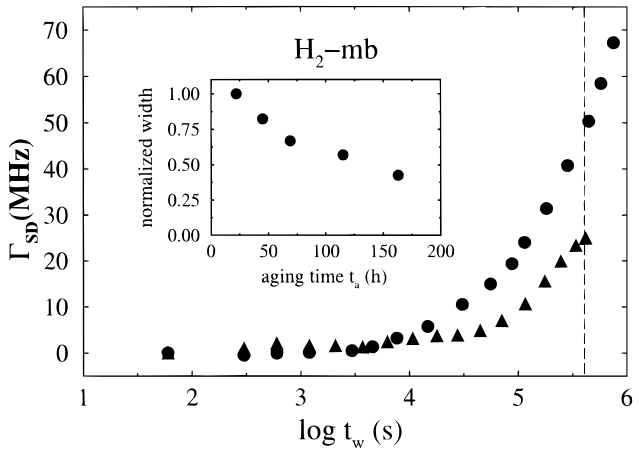

Figure 7. Spectral diffusion broadening for H_2-mb, for two different aging times ($t_{a1} = 22$ h, $t_{a2} = 115$ h). The time origin is defined as the time where the system had reached the experimental temperature of 100 mK for the first time. The inset shows how spectral diffusion broadening decays as a function of aging time for a fixed waiting time of 5×10^5 s.

be concluded from additional line broadening in the millisecond region. Also, the line broadening associated with feature *c* eventually levels off, at 8.1 K, from which we conclude that feature *c* is also relatively narrow and is shifting as a function of temperature. The data at 12 K clearly show that feature *c* has shifted further in the direction of larger fluctuation rates, resulting in a very pronounced plateau in the region between 0.1 and 100 ms. However, no evidence for a fourth feature is observed until 23 K. Although the scatter in the data is much worse than at the lower temperatures, the data at 23 K clearly show an increase of the line width in the millisecond region. An important point is that each subsequent feature causes the line width to broaden by a larger amount than the previous feature. Since the magnitude of the line broadening is related to the accessible volume of the conformational phase space, we can conclude not only that the protein explores its conformational phase space in discrete steps but also that each subsequent step corresponds to a larger region of phase space.

A fascinating picture emerges when we plot the temperature dependence of the fluctuation rates corresponding with the central rate of each of the three distributions, *a*, *b*, and *c*, as is done in Figure 5. From Figure 5 we can deduce that the temperature dependence of all three features follow an Arrhenius law, suggesting that also the conformational changes associated with features *b* and *c* occur via thermally activated barrier crossing. However, since the preexponential factors are rather small, a possible tunneling contribution to the fluctuation rate cannot be excluded. The thermodynamic parameters that result from linear fits to the data in Figure 5 are listed in Table 1. We observe that each subsequent feature that contributes to the line broadening corresponds to a larger barrier height and that all features exhibit roughly the same preexponential factor of 10^7. Although we did not perform a temperature dependent study for the fourth feature, we can make a rough estimate of the energy barrier corresponding to this feature by assuming the same preexponential. From this we find a barrier of approximately 3 kJ mol^{-1}; therefore, a pronounced gap in the distribution of energy barriers exists between 0.6 and 3 kJ mol^{-1}.

C. Aging Time Experiments: How Close to Equilibrium Is the Protein at 100 mK? For the experiments in the millikelvin range we checked explicitly whether the protein was in thermal equilibrium. Figure 7 shows an aging time SD experiment for H_2-mb. The line broadening as a function of t_w is characterized by two distinct regimes. An initial period of a few hours where broadening is weak is followed by a regime where broadening is strong. However, it is quite clear that the broadening at longer times is caused by a nonequilibrium phenomenon because it ceases with t_a. The inset in Figure 7 shows how the line width at $t_w = 5 \times 10^5$ s decays as a function of t_a. We observe that after an aging time of roughly one week the decay levels off and, hence, the protein must be in (local) equilibrium. Three points should be stressed within this context. First, what we refer to as equilibrium is not necessarily a global character. There may be lower minima separated by barriers that cannot be surpassed at liquid helium temperatures, at least not on the time scale of our experiments, which is a few hundred hours. Therefore, these barriers do not influence the relaxation behavior. Second, it is not necessary for the broadening in Figure 7 to decay to zero because in addition to the nonequilibrium processes, there may be also equilibrium phenomena that determine the final value of the line width. Third, we also performed aging time SD experiments at 4 K. At this temperature there is no dependence of the SD on t_a, and hence, the protein must be in equilibrium in the sense discussed above.

TABLE 1: Thermodynamic Parameters for Conformational Fluctuations of Myoglobin

	a	*b*	*c*
E (kJ mol^{-1})	0.20	0.38	0.57
A (s^{-1})	2×10^6	1×10^7	4×10^6

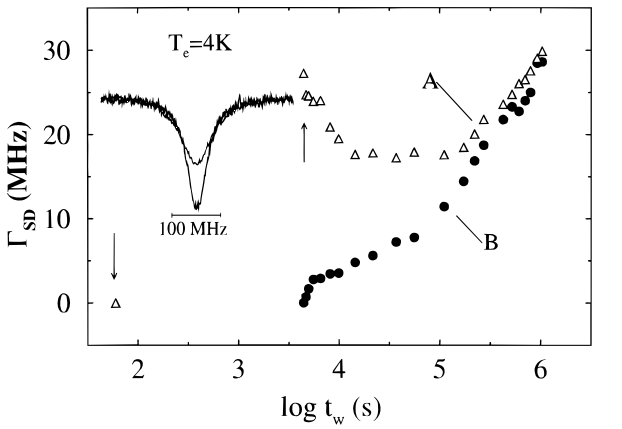

Figure 8. Combination of a temperature cycle and a waiting time experiment: Hole A was burned immediately before the temperature cycle, however, after a relaxation period t_a of 10 days. The inset shows hole A at the waiting times marked by arrows, i.e. immediately before and after the temperature cycle. Hole B was burned immediately after the cycle. Excursion temperature $T_e = 4$ K, experimental temperature 100 mK. Sample: H_2-mb.

D. Temperature Cycle Induced Spectral Diffusion. Figure 8 shows the results of a temperature cycle experiment, where the width of two spectral holes, A and B, was studied as a function of t_w. Before performing the experiment the sample was cooled down to 100 mK and was allowed to relax for approximately 250 h. From the aging time experiments we know that after 250 h the protein has established a local equilibrium. After this period hole A was burned, which serves as a marker of the equilibrium state of the sample. After hole A was burned the sample was exposed to a temperature cycle with $T_e = 4$ K and $t_e = 80$ min. Immediately after the cycle hole B was burned, which is the marker of the protein in its nonequilibrium state. The experiment was repeated for $T_e = 8$ K, but no significantly different behavior was found. To stress the specific behavior of a protein in this experiment, a comparative experiment was performed on the same chromophore in a glass of glycerol and dimethylformamide, the results of which are shown in Figure 9. In the case of the

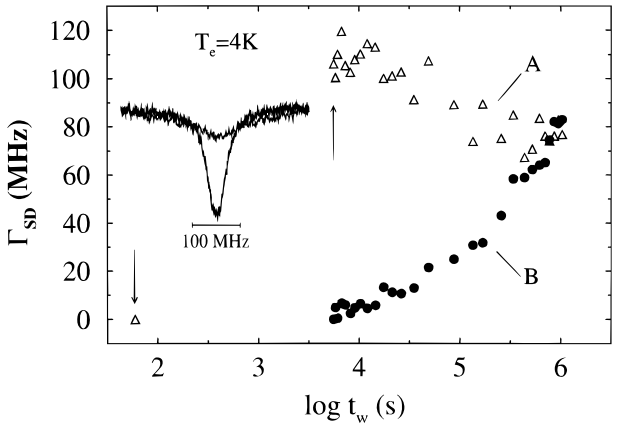

Figure 9. Same experiment as Figure 8, however without apoprotein. Protoporphyrin IX is directly dissolved in a glycerol/dimethylformamide glass.

protein, immediately after the cycle, hole A has broadened with respect to its initial width because during the cycle the protein has explored a larger part of its conformational phase space than is accessible at 100 mK. Afterward, it runs through a time regime where it narrows considerably. This regime lasts for approximately 10 h, after which line broadening takes over. During the period that hole A narrows, hole B broadens by roughly the same amount. An interesting observation is the asymptotic behavior of the two holes. According to our data the two traces approach each other, but they do not cross. For the glass the situation is drastically different. The narrowing regime for hole A persists throughout the whole experimental period without any indication of a minimum, and contrary to the protein, traces A and B do cross.

Since we do not have a tractable model for the EL of a protein, we start the discussion of these results with the simplest model available, the TLS model.[19,27] The line broadening, Γ, induced by the fluctuations of an ensemble of TLSs is proportional to the number of TLSs that have changed their state during a certain time, t. This number, in turn, is proportional to the conditional probability that a TLS, initially being in the upper state, will be found in the lower state, and vice versa. Hence, in thermal equilibrium, Γ is given by

$$\Gamma \propto \langle P(T)[1 - P(T)][1 - P(T)][1 - \exp(-Rt)]\rangle \quad (4)$$

where $P(T)$, the probability of finding a TLS with an energy splitting, ϵ, between its upper and lower state, is given by

$$P(T) = 1/[1 + \exp(\epsilon/kT)] \quad (5)$$

The brackets indicate an average over the TLSs in the ensemble. Note that eq 4 merely reflects the entropy change during the period t. In order to describe a temperature cycle experiment, eq 4 needs to be modified. We need to consider three temperatures, the initial temperature, T_i, the excursion temperature, T_e, and the final temperature, T_f. In our case $T_i = T_f =$ 100 mK and $T_e = 4$ and 8 K, respectively. In this case, we can write for hole B

$$\Gamma_B \propto f_{ie}(t_w) \quad (6)$$

and for hole A

$$\Gamma_A \propto f_{ie}(\infty) + f_{ii}(t_w) - f_{ie}(t_w) \quad (7)$$

with

$$f_{ab} = \langle P(T_a)[1 - P(T_b)] + P(T_b)[1 - P(T_a)][1 - \exp(-Rt_w)]\rangle \quad (8)$$

where t_w is the waiting time *after* the temperature cycle. For $T_e > T_i$ one can show that Γ_A decreases monotonically, that $\Gamma_A(0) > \Gamma_B(t_w)$, and that $\Gamma_A(\infty) < \Gamma_B(\infty)$. These conclusions hold for any distribution of TLS parameters.[19] The most important consequences pertaining to the results of Figures 8 and 9 are that $\Gamma_B(t_w)$ can never exceed $\Gamma_A(0)$ and that $\Gamma_A(t_w)$ and $\Gamma_B(t_w)$ have to cross at some point. The experimental results for the glass comply with all these conclusions, whereas the data for the protein violate all. The obvious conclusion is that while the TLS model properly describes SD in glasses, it does not do justice to the complex features of the EL of a protein. In the next section we will show that, in order to understand the results from the various types of experiments presented in this section, one needs to consider the global features of the EL.

5. The Structure of the Energy Landscape

In the previous section we have seen that the SD behavior in myoglobin exhibits a number of very specific features. We observed stepwise line broadening between 1.7 and 23 K, nonequilibrium effects at 100 mK, and reversible line broadening after well-defined temperature cycles. In the latter case, comparative experiments on a glass showed both quantitatively and qualitatively different behavior that most likely originates from differences between the ELs of proteins and glasses. While the TLS model seems to give a proper description of the optical dynamics of a chromophore doped into a glass, it fails when the chromophore is an intrinsic part of a protein. The purpose of this section is to arrive at a formal description of a protein EL that does agree with the experimental results presented here and is in general agreement with present views.

We start the analysis with the discussion of the temperature cycle SD experiments presented in section 4D. In these experiments we observed that the line broadening induced by temperature cycles to 4 and 8 K is partly reversed over a period of several hours after the cycle. To explain this result, we consider an EL that is described by a single well with a rough structure superimposed on it, as is shown in Figure 10 a. The steepness of the well is such that, at 100 mK, only the lowest energy state is populated. During the temperature cycle each protein starts to access local minima of higher energy, and after a certain time the distribution of the ensemble of proteins over the local minima satisfies thermal equilibrium conditions. Hence, if the temperature is lowered again to 100 mK, the ensemble is in a nonequilibrium state. Reestablishment of thermal equilibrium, i.e. repopulation of the lowest energy state, will take considerable time because of the roughness of the potential. Within this model, we expect hole A to have broadened when its width is measured immediately after the temperature cycle because the protein has explored its conformational phase space during the cycle. After the cycle, we expect hole A to slowly relax to its original width because each protein returns to its original point in phase space and, therefore, also to the same point in frequency space. Consequently, hole *B* should broaden by the same amount and on the same time scale as hole A narrows, since it was burned when the ensemble was in the nonequilibrium state, right *after* the temperature cycle. However, the time evolution of the two holes is determined by exactly the same processes. Their different behavior is merely caused by the fact that they were burned in different (non)-equilibrium states. This picture is only in qualitative agreement with the experimental results. Indeed hole A narrows while hole B broadens by the same amount, but hole A relaxes to a

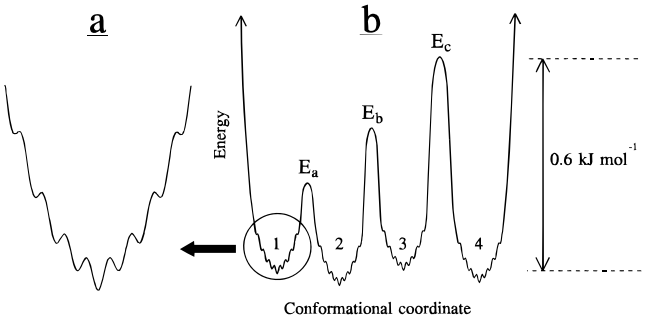

Figure 10. Schematic representation of the energy landscape of myoglobin in the region up to 1 kJ mol^{-1} based on the results presented.

value that is larger than its original width. The reason for this discrepancy is that the representation of the overall shape of the potential as a single well is not correct. Instead of a single lowest energy state there are a number of almost degenerate local minima, i.e. CSs, that are separated by barriers that are large compared to the roughness on the potential. This is illustrated in Figure 10b. During the temperature cycle the ensemble of proteins has access to these CSs so that only a subpopulation of the ensemble returns to its original state. The width of hole A, immediately after the cycle, contains a nonreversible contribution from the subpopulation that ends up in a different CS and a reversible contribution due to the subpopulation that returns to the same state from which it originated. Since the narrowing of hole A is still quite substantial, approximately one-third of the initial broadening, this means that the probability of returning to the same CS is quite large and, hence, that the number of accessible CSs is small, typically on the order of three.

From the 3PSE experiments we obtained barriers of 0.2, 0.4, and 0.6 kJ mol^{-1} with a preexponential factor of approximately 10^7. We now denote these as E_a, E_b, and E_c, respectively. Before we discuss how these barriers fit within the model of the EL, we need to check whether the thermodynamic parameters agree with the nonreversible broadening observed in the temperature cycle experiments. In order to contribute to the temperature cycle induced broadening, a structural rearrangement should occur on a time scale longer than t_e at 100 mK and on a time scale comparable to or shorter than t_e at T_e. This is true for the features *a*, *b*, and *c* observed in the 3PSE experiments, for both $T_e = 4$ and 8 K. However, the fourth feature will not contribute since its rate is on the order of 10^{-9} s^{-1}, even at 8 K. Hence, the 3PSE experiments and the temperature cycling hole burning experiments are in complete agreement, where the identical behavior for $T_e = 4$ and 8 K is due to the absence of barriers between 0.6 and 3 kJ mol^{-1}.

Recently, we attributed E_a, E_b, and E_c to individual tiers within a hierarchically organized EL.[28] However, this view needs to be adjusted in light of the temperature-cycling SD experiments. During a temperature cycle to 4 K, E_a, E_b, and E_c can be crossed. If each of these three barriers represents a hierarchical tier comprising N states, the probability of returning to the original state is $1/N^3$. Therefore, even if N is a small number, this probability is quite small. However, the reversibility of the temperature cycle induced broadening indicates that this probability must be on the order of 1/3. An alternative explanation is that each protein resides in a local minimum containing a small number CSs, such as the one shown in Figure 10b. In this case, the barriers E_a, E_b, and E_c are the energy barriers separating these states. We can imagine that there are four CSs along a single coordinate, which gives three possible arrangements of the energy barriers, only one of which is shown in Figure 10b. Such an arrangement implies that only transitions between adjacent CSs are possible. For instance, in order to go from CS 1 to CS 4 the protein has to go via CSs 2 and 3. We can also imagine that there are three states all of which are mutually connected by a single barrier, that is, direct transitions between all three CSs are possible.

One of the arguments to assign the three features of the 3PSE-experiments to different hierarchical tiers was that each subsequent feature *a*, *b*, and *c* corresponded to a higher barrier but also exhibited stronger SD broadening than the previous feature. The amount of broadening is related to the amplitude of the corresponding structural rearrangement. The logical conclusion was that each subsequent feature corresponds to protein motions with increased amplitude, much in agreement with the hierarchical picture. As it turns out, we can explain the same effect in terms of the alternative model of Figure 10b. We consider the arrangement of Figure 10b, where all four CSs are equally populated. At a given temperature, a spectral hole is burned at $t_w = 0$. When t_w approaches the inverse of the rate, R_a, of crossing barrier E_a, between CSs 1 and 2, the hole will broaden due to transitions between these two CSs. The broadening is properly described by a single TLS if the rate, R_b, of crossing barrier E_b between states 2 and 3 is much smaller than R_a. Only the subpopulation of proteins that were in either state 2 or 3 at $t_w = 0$ will contribute to the broadening. However, when t_w is increased so that it approaches $1/R_b$, additional SD occurs because now CSs 2 and 3 can interchange. But, at this point also CSs 1 and 3 are connected, which gives an extra contribution to the SD. When t_w is further increased so that also the barrier, E_c, between CS 3 and 4 is crossed, not only states 3 and 4 but all four states become connected. If we assume that the SD broadening induced by going from one CS to another is proportional to the distance between these two states along the conformational coordinate, i.e. the increase in accessible phase space volume, one can show that the amount of SD should increase by a factor of approximately 1.5 for each subsequent feature,[29] which is in excellent agreement with the experimental results. However, this only holds for the arrangement shown in Figure 10b and the arrangement with E_b as central barrier. For the arrangement with E_c as central barrier, features *a* and *b* will give the same amount of broadening, while feature *c* should exhibit an approximately 4-fold increase. The three-state model can be easily refuted. In this case crossing only the first two barriers induces SD. Crossing the third barrier does not add to the line broadening because all CSs were already connected by the first two barriers. Hence, in this case, only two features instead of three should be observed.

Now that we have established that the potential energy surface drawn in Figure 10b represents a part of the EL of the protein, the next step is to find out how this part of the EL fits within the overall structure of the energy surface. A first question that arises is whether the four CSs are part of an absolute or a local minimum within the EL. There are two simple arguments that show that we must be dealing with a local minimum. The first argument involves the amount of line broadening as compared to the total width of the absorption spectrum. The total amount of line broadening induced by the transitions between the four CSs is approximately 0.05 cm^{-1}, while the width of the spectrum is approximately 600 cm^{-1}. Since the spectral width is a measure of the phase space volume occupied by the protein, this means that the protein can adopt many more CSs than the four shown in Figure 10b, and therefore, there must be a large number of additional local minima. The same conclusion can be drawn from the fact that the line broadening is reactivated at 23 K and from temperature cycle experiments by Shibata et al.[30] Both of these results indicate that there are a small number

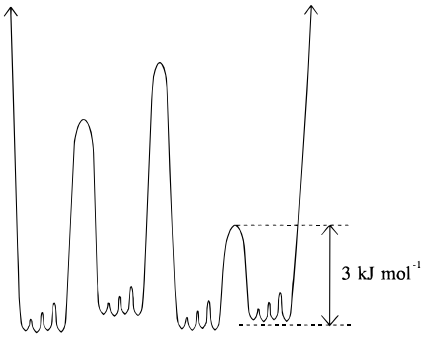

Figure 11. Schematic representation of the energy landscape of myoglobin in the region up to 10 kJ mol^{-1} based on the results presented.

of energy barriers, between 3 and 10 kJ mol^{-1}, to additional local minima.

The next question that arises is how it can be that although the energy surface displayed in Figure 10b corresponds to only one of several local minima, it is still represented by such salient experimental features. One explanation is that the energy surface of Figure 10 b represents four possible conformations of a restricted region of the protein, i.e. a spatially localized minimum, similar to the TLS model. However, this leaves the question why these spatially localized CSs are not observed in the other structural regions of the protein. An alternative explanation is that the structure of Figure 10b is repeated within each local minimum, as is shown in Figure 11. This brings us back to the concept of a hierarchical organization of the EL. It is well-known that on the highest hierarchical tier approximately three CSs, the so-called taxonomic CSs exist.[22] These could be observed in the absorption spectrum of Figure 3. An intriguing observation is that we found the same number of CSs, however, on a much smaller scale, in terms of both energy and phase space volume. A possibility that should be taken into consideration is that each CSs on a certain hierarchical tier is split into a small number, typically of the order of four CSs of a lower hierarchical tier. Comparing the barriers E_a, E_b, and E_c to the barriers between the taxonomic CSs, which are on the order of 10^2 kJ mol^{-1},[31] and comparing the observed line broadening to the width of the absorption spectrum, we must conclude that there are a number of tiers between the taxonomic CSs and the ones displayed in Figure 10b. The 3PSE experiments supplied evidence for a fourth barrier, and so automatically, the question arises how this barrier is related to the organization of the EL. A first clue is that the barrier of approximately 3 kJ mol^{-1} is almost an order of magnitude larger than the average barrier found at the lower temperatures. Therefore, it most likely belongs to a higher tier. We emphasize that an increase of the barrier height of slightly less that an order of magnitude would give a total number of tiers of approximately four, which is in excellent agreement with the model proposed by Frauenfelder and co-workers.[7] Another clue that supports that the SD induced by the fourth feature is due to transitions between CSs within a higher tier is that the amount of line broadening induced by the fourth feature is at least 3 times as strong as feature *c*. If the fourth barrier would merely correspond to a fifth state within a local minimum, the amount of broadening would have been much smaller. There is strong evidence that the number of CSs within this tier is also quite small. The temperature cycle induced broadening measured by Shibata et al.[30] occurs as a stepwise function of T_e, between $T_e = 15$ and 70 K. Analogous to the stepwise line broadening observed in the 3PSE experiments, this implies that the distribution of energy barriers between the CSs within this tier is pseudodiscrete and, hence, that the number of CSs is small.

6. Summary and Outlook

Optical line narrowing methods provide insight into the complex features of the energy landscape of a protein. By combining the results of a series of photon echo and spectral hole burning experiments, we construct an image of the low-energy part of the EL of myoglobin with a degree of detail that has not been realized before. These experiments give quantitative information about the height and distribution of the energy barriers between the CSs of the protein as well as give insight into the overall organization of the EL. The most important conclusions are the following.

1. The slow relaxation toward thermal equilibrium at low temperature (100 mK), measured in aging time and temperature cycle SD experiments, points toward the presence of a rough structure superimposed on the overall shape of the EL.

2. The stepwise line broadening observed in 3PSE experiments between 1.7 and 23 K and in temperature cycle hole-burning experiments between 15 and 70 K shows that the distribution of energy barriers between the CSs of the protein comprises a number of discrete features: three features between 0.2 and 0.6 kJ mol^{-1} and approximately three features between 3 and 10 kJ mol ^{1}. These results are in agreement with a hierarchical organization of the EL, but in a different way than was previously anticipated. A careful analysis of both photon echo and hole burning results shows that the three features observed between 0.2 and 0.6 kJ mol^{-1} belong to the same hierarchical tier, rather than to different hierarchical tiers, as was recently proposed.[28] The transition to the next hierarchical tier is indicated by the gap in the distribution of energy barriers between 0.6 and 3 kJ mol^{-1}, as is confirmed by a large increase in the amount of line broadening.

3. The number of CSs in the lower hierarchical tiers appears to be much lower than was previously suggested.[32] For the lowest tier we find four CSs, comparable to the number of taxonomic substates. We propose that each CS in a given hierarchical tier is split into a small number, on the order of four, of CSs on the next lower level. From the increase in barrier height between the CSs in the lowest tier and the next higher tier we estimate the total numbers of tiers to be four, in excellent agreement with the model proposed by Frauenfelder and co-workers.[7]

Although the experiments paint a highly detailed picture, our understanding of protein dynamics and ELs is still rudimentary. For instance, the nature of the conformational fluctuations remains unknown. Apart from developing new experimental and theoretical probes, this point may be addressed by performing experiments on selectively mutated proteins. Another important question is whether these results are specific to myoglobin or may provide a general framework to describe the ELs of proteins. The methods that were used are generally applicable to chromoproteins, and the results of preliminary experiments on cytochrome *c* and horseradish peroxidase are looking promising.[26,33,34]

Acknowledgment. D.T.L. and D.A.W. acknowledge J. M. Vanderkooi, A. A. van Dijk, and G. T. Robillard for their assistance with sample preparation, H. Frauenfelder for stimulating discussions, and the Netherlands Foundation for Physical Research (FOM) and the Netherlands Organization for Scientific Research (NWO) for financial support. K.F. and J.F. acknowledge the DFG (SFB 279,C2, Graduiertenkolleg "Nichtlineare Dynamik und Spektroskopie") and the Fonds der Chemischen Industrie for support and F. Parak, J. L. Skinner, and J. M. Vanderkooi for helpful discussions.

References and Notes

(1) Austin, R. H.; Beeson, K. W.; Eisenstein, L.; Frauenfelder, H.; Gunsalus, I. C. *Biochemistry*, **1975**, *14*, 5355.

(2) For a recent review see: Dill, K. A.; Chan, H. S. *Nature Struct. Biol.* **1997**, *4*, 10.

(3) Frauenfelder, H.; Petsko, G. A.; Tsernoglou, D. *Nature* **1979**, *280*, 558.

(4) Campbell, B. F.; Chance, M. R.; Friedman, J. M. *Science* **1987**, *238*, 373.

(5) Thorn Leeson, D.; Berg, O.; Wiersma, D. A. *J. Phys. Chem.* **1994**, *98*, 3913.

(6) Denisov, V. P.; Peters, J.; Hörlein, H. D.; Halle, B. *Nature Struct. Biol.* **1996**, *3*, 505.

(7) Ansari, A.; Berendzen, J.; Bowne, S. F.; Frauenfelder, H.; Iben, I. E. T.; Sauke, T. B.; Shyamsunder, E.; Young, R. D. *Proc. Natl. Acad. Sci. U.S.A.* **1985**, *82*, 5000.

(8) Friedrich, J. In *Methods of Enzymology*; Sauer, K., Ed.; Academic: San Diego, Vol. 246, pp 226−259.

(9) Wiersma, D. A.; Duppen, K. *Science* **1987**, *237*, 1147.

(10) Bai, Y. S.; Fayer, M. D. *Phys. Rev. B.* **1989**, *39*, 11066.

(11) Hu, P.; Walker, L. R. *Phys. Rev. B.* **1978**, *18*, 1300.

(12) Anderson, P. W.; Halperin, B. I.; Varma, C. M. *Philos. Mag.* **1972**, *25*, 1.

(13) Phillips, W. A. *J. Low Temp. Phys.* **1972**, *7*, 351.

(14) A good review is: Narasimhan, L. R.; Littau, K. A.; Pack, D. W.; Bai, Y. S.; Elschner, A.; Fayer, M. D. *Chem. Rev.* **1990**, *90*, 439.

(15) Singh, G. P.; Schink, H. J.; v. Löhneysen, H.; Parak, F.; Hunklinger, S. *Z. Phys. B.* **1984**, *55*, 23.

(16) Rella, C. W.; Kwok, A. S.; Rector, K. D.; Hill, J. R.; Schwettman, H. A.; Dlott, D. D.; Fayer, M. D. *Phys. Rev. Lett.* **1996,** *77*, 1648.

(17) Rella, C. W.; Rector, K. D.; Kwok, A. S.; Hill, J. R.; Schwettman, H. A.; Dlott, D. D.; Fayer, M. D. *J. Phys. Chem.* **1996**, *100*, 15620.

(18) Kurita, A.; Sibata, Y.; Kushida, T. *Phys. Rev. Lett.* **1995**, *74*, 4349.

(19) Fritsch, K.; Friedrich, J.; Parak, F.; Skinner, J. L. *Proc. Natl. Acad. Sci. U.S.A.* **1996**, *93*, 15141.

(20) Meijers, H. C.; Wiersma, D. A. *J. Chem. Phys.* **1994**, *101*, 6927.

(21) Gafert, J.; Ober, C.; Orth, K.; Friedrich, J. *J. Phys. Chem.* **1995**, *99*, 14561.

(22) Ansari, A.; Berendzen, J.; Braunstein, D.; Cowen, B. R.; Frauenfelder, H.; Hong, M. K.; Iben, I. E. T.; Johnson, J. B.; Ormos, P.; Sauke, T. B.; Scholl, R.; Schulte, A.; Steinbach, P. J.; Vittitow, J.; Young, R. D. *Biophys. Chem.* **1987**, *26*, 337.

(23) Gafert, J.; Friedrich, J.; Vanderkooi, J.; Fidy, J. *J. Phys. Chem.* **1995**, *99*, 5223.

(24) Gafert, J.; Friedrich, J; Parak, F. *Proc. Natl. Acad. Sci U.S.A.* **1995**, *92*, 2116.

(25) See the results of Figures 8 and 9.

(26) Thorn Leeson, D.; Wiersma, D. A. *Phys. Rev. Lett.* **1995**, *74*, 2138.

(27) Fritsch, K.; Friedrich, J.; Kharlamov, B. M. *J. Chem. Phys.* **1996**, *105*, 1798.

(28) Thorn Leeson, D.; Wiersma, D. A. *Nature Struct. Biol.* **1995**, *2*, 849.

(29) We assume that the total amount of SD is proportional to the fraction of proteins that have gone from one CS to another times the distance, *d*, between these two CSs along the conformational coordinate. The distance between two adjacent CSs is defined as *x*. For $1/R_b,R_c >> t_w >> 1/R_a$, $SD_{tot} = (1/2)d(1\rightarrow2) + (1/2)d(2\rightarrow1) = x$. This is the amount of SD induced by feature *a*. For $1/R_c >> t_w >> 1/R_a,R_b$, $SD_{tot} = (1/3)d(1\rightarrow2) + (1/3)d(1\rightarrow3) + (1/3)d(2\rightarrow1) + (1/3)d(2\rightarrow3) + (1/3)d(3\rightarrow1) + (1/3)d(3\rightarrow2) = 2.67x$. This the amount of SD induced by features *a* and *b*. The amount of spectral diffusion induced by feature *b* is therefore $1.67x$. Along the same lines we find that the amount of SD induced by feature *c* is equal to $2.33x$.

(30) Shibata, Y.; Kurita, A.; Kushida, T., *J. Chem. Phys.* **1996**, *104*, 4396.

(31) Johnson, J. B.; Lamb, D. C.; Frauenfelder, H.; Müller, J. D.; McMahon, B.; Nienhaus, G. U.; Young, R. D. *Biophys. J.* **1996**, *71*, 1563.

(32) Frauenfelder, H.; Sligar, S. G.; Wolynes, P. *Science* **1991**, *254*, 1598.

(33) Zollfrank, J.; Friedrich, J.; Vanderkooi, J. M.; Fidy, J. *Biophys. J.* **1991**, *59*, 305.

(34) Fritsch, K.; Friedrich, J. To be published.